Experimental investigations and model study of moisture behaviors in polymeric materials

X.J. Fan [a,c,*] *

1. A conventional underfill. The sample is a disk shape with a diameter of 50 mm and a thickness of 1 mm. Moisture absorption under 85 °C/85% RH was performed.
2. A thin bismaleimide-triazine (BT) core material. 7 mm × 7 mm with a thickness of 70 μm. In this study, moisture absorption–desorption experiments were performed at 30, 60, and 80 °C, respectively. At each isothermal temperature, two relative humidity levels were chosen: 60% and 80% RH, respectively. In situ measurement was performed for this thin sample [11].
3. A thick bismaleimide-triazine (BT) core material. The sample size is 50 mm × 50 mm with a thickness of 0.6 mm. Moisture absorption was performed under 30 °C/60% RH.
4. A conventional mold compound: two different sample geometries both from the same material in the form of molded disks were produced with the thickness of 1 mm (MC1) having a diameter of 50 mm and the samples with the thickness 2 mm (MC2) having a diameter of 100 mm, respectively. They were then exposed to the 85 °C/85% RH conditions in a humidity chamber [12].

To determine the dry weights, the samples were dried initially at 125 °C for 24 h. An electronic balance scale was used for the weight gain measurements except for the thin BT core, in which

From the Fig. 1, it can be seen that the Fick's diffusion law predicts the experimental behavior very well within the tested period. With increasing , the absorption curve smoothly levels off to a saturation level ∞. Our previously tested results on different types of underfill also exhibited Fickian behaviors [3].

Fig. 2 shows an example of moisture absorption–desorption experiment for a thin BT core, where the temperature was kept

at 60 °C and the RH level was cycled between 0% and 60%. During the first 60 min, a 0% RH condition was imposed to drive any residual moisture out of the sample. This was followed by a 200 min of moisture absorption at 60% RH, then a 200 min desorption at 0% RH.

Based on the results from Fig. 2, several points are clear: (1) during the first 60 min, the moisture was not completely driven out of the sample, a longer time was needed to accomplish that; (2) the subsequent absorption–desorption cycles were repeatable, i.e., the sample reached approximately the same saturated moisture level during sorption and it lost the same weight upon drying. This indicates that there is no chemical reaction between the water molecules and the material. However, as shown in Fig. 3, the Fickian fit is not satisfactory. This might be due to the fact that the BT core has a highly inhomogeneous structure involving glass fibers and resin matrix.

Fig. 4 is a plot of the moisture weight gain for a thick BT core with a thickness of 0.6 mm at 30 °C/60% RH. After the extended hours of moisture absorption, the moisture uptake starts to increase again. It clearly shows the two-stage moisture absorption. The material behaves initially as Fickian's behavior, followed by a non-Fickian diffusion behavior.

The moisture absorption for a mold compound is plotted in Fig. 5 with two different thicknesses. An initial moisture uptake to quasi-equilibrium (the first stage of 'virtual' saturation) is followed by a slower linear moisture uptake. This suggests that at least two different mechanisms are available in the moisture absorption. The first mechanism is the absorption of water

Fig. 1. Fickian curve fit for a homogeneous underfill material under 85 °C/85% RH (sample size 50 mm × 50 mm × 1 mm).

molecules in free-volumes or nano-voids. The second mechanism is the hydrogen bonding formation between the water molecules and polymer chains due to their molecular polarity. The former mechanism reaches a saturation point and is a reversible phenomenon in nature. The latter seems to be linear without a clear saturation, at least for the time scales reported in this study. The

data were obtained from moisture absorption–desorption experiments. It clearly shows that ___ in BT core is essentially temperature independent.

For most polymer materials at the temperature well below the glass transition temperature, ___ is independent of temperature. This implies that the solubility decreases with temperature according to Eq. (16). However, the situation will be different when the temperature is across the glass transition temperature (T_g). Fig. 8 plots the saturated moisture concentration for a die-attach film as a function of temperature in a range from 30 to 80 °C at 60% RH level. It shows a strong dependency with temperature. This film has a T_g around 35 °C. It reveals that in the temperature region across the T_g, the saturated moisture concentration depends strongly on the temperature. As a matter of fact, since the saturated moisture concentration has strong dependency on the free volume fraction, it is suggested that the saturated moisture concentration will increase significantly when temperature goes across the glass transition temperature. It becomes very important to investigate the saturated moisture concentration at reflow temperature since an 'over-saturation' phenomenon will be observed at the reflow [16,17]. Over-saturation refers to a situation that a material might continue to absorb more moisture despite that desorption takes places during soldering reflow. When saturated moisture concentration is a function of temperature, the moisture diffusion modeling using normalization approach is no longer valid [3]. A direct moisture concentration (DCA) has been proposed to conduct moisture diffusion modeling at reflow process [16,17].

4. Water sorption and moisture sorption

When a polymer material is immersed into water, the sorption process is referred to as water sorption. For a material that is subjected to a humid air condition with a relative humidity less than 100%, it is referred to as moisture sorption process. There are two distinct diffusion mechanisms involved in the transport of moisture: transfers across surface and through bulk, respectively. Moisture diffusion mechanism across surface has not been clear [18]. In order to study the difference for water sorption versus moisture sorption, an experiment of moisture weight gain test and sensitivity/reflow test for two groups of QFN packages was conducted. One group of QFN packages was coated with a hydrophobic membrane, which was formulated by a grafting method [19], to prevent water uptake, while the other group was as received. Two types of moisture preconditioning were applied: immersion into water at a constant temperature of 60 °C, and placement in a humidity chamber at 60 °C/85% RH. Both sorption
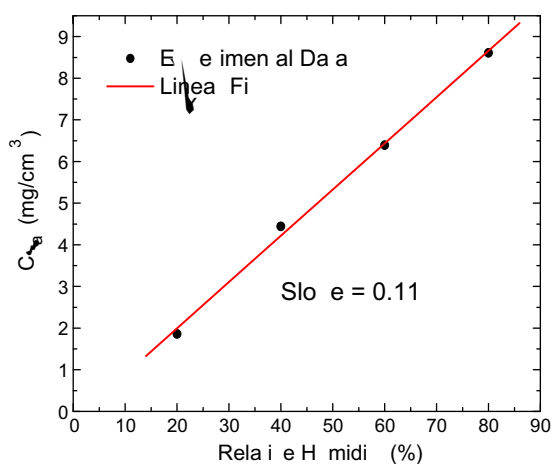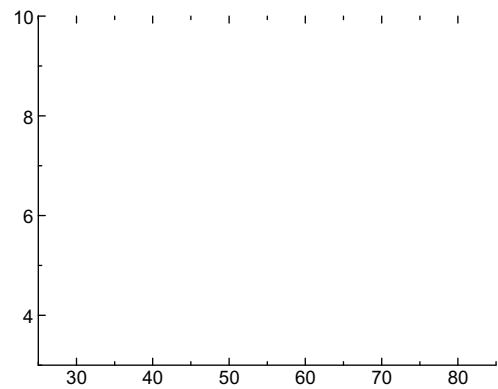
Fig. 6. ___ as a function of relative humidity at 30 °C [11].

durations were 192 h. Table 1 summarizes the weight gain test data and the results after the reflow. The coated packages under water did not have any weight change. However, the coated packages in humid air condition gained almost the same amount of moisture compared to the uncoated packages either in water or in humid air. Further, the reflow test indicates that the coated packages at 60 °C/85% RH preconditioning had the same failure rate with the uncoated in the same preconditioning conditions, while the coated packages immersed under water did not show any failures after the reflow. These results imply that a hydrophobic polymer film is very effective in blocking water liquid from penetrating through surface, but not for water vapor transmission (see Fig. 9). Several other hydrophobic polymeric materials have been found to exhibit the similar phenomenon of water vapor passage in humid air conditions [20]. More studies are needed to understand the surface diffusion mechanism. Throughout this paper, unless it is stated, the moisture absorption process is generally assumed.

5. Characterization of pore size, porosity and free volume

Porosity or free volume fraction of polymers are critical material properties related to moisture absorption. Polymer volume is divided into three elements: occupied volume (the "van der Waals" volume), interstitial free volume, and hole-free volume [21,22]. The hole-free volume is accessible for penetrant transport, and may be altered by absorption and desorption of penetrants.

Several types of polymer materials in packaging applications, such as die-attach films, solder mask, and underfills, were tested using Mercury intrusion [23]. Those materials were also examined for moisture weight gain test at 85 °C/85% RH. The results showed that the relative weight gain ranged from 0.48% to 1.27% for those tested materials. However, no significant pore size down to ~50 nm was observed for all materials. This implies that the free-volumes, which are occupied by the absorbed moisture, are typically in nanometer range. The same materials were then subjected to a simulated reflow process. Fig. 10 shows an example of microstructures of a die-attach film before and after the reflow. It can be seen that the significant voiding of film due to internal vapor pressure was developed after the reflow process [24]. Soles et al. [25] used Positron Annihilation Lifetime Spectroscopy (PALS) to quantify the polymer network topology, which produces a nanovoid volume fraction as a function of temperature. A strong correlation was observed between the absolute zero volume fraction and the ultimate moisture uptake. Although the correlation is clear, the absolute moisture zero hole volume fraction is not suffi-
(1-)]TJ0-23-299(06T871%ict0(re-302(r22imate)-556(to)-ture)-296(3-29ke.)-5

Changes in the total polymer volume are largely governed by changes in the hole-free volume.

Mercury intrusion porosimetry characterizes a material's porosity by applying various levels of pressure to a sample immersed in mercury [23]. The pressure required to intrude the mercury into sample's pores is inversely proportional to the size of pores. Mercury porosimetry is based on the capillary law governing liquid penetration into small pores. This law, in the case of a non-wetting liquid like mercury, is expressed by the Washburn's equation

$$D = \frac{-4\gamma \cos\theta}{} \tag{17}$$

where γ is surface tension of mercury, θ is the contact angle between the mercury and the sample, is the applied pressure, and D is the pore diameter, all in consistent units. The volume of mercury penetrating the pores is measured directly as a function of applied pressure. This – information serves as a unique characterization of pore structure. The Washburn equation assumes that all pores are cylindrical. Although pores or free-volumes are rarely cylindrical in reality, this equation provides a practical representation of pore distributions, yielding very useful results for most applications. As pressure increases during an analysis, pore size is calculated for each pressure point, and the corresponding volume of mercury required to fill these pores is measured. These measurements taken over a range of pressures give the pore volume versus pore size distribution for the sample material. Mercury porosimetry can determine pore size distribution accurately. Comprehensive data provide extensive characterization of sample porosity and density. Available results include total pore volume, pore size distribution and pore diameter. In general, mercury porosimetry is applied over a capillary diameter range from 50 nm to 360 μm.

Since the density of the liquid water is 1.0 g/cm^3, the moisture density in free volume, i.e., ρ in Eq. (18), must be less than or equal to 1.0 g/cm^3,

$$_0 \geq \quad . \tag{19}$$

when the _____ uses the unit of g/cm^3. In general, the $_{sat}$ depends on the relative humidity and temperature. It has been suggested that the water liquid will fill in the free volume completely at 100% RH [26,27]. Therefore the initial free volume fraction can 50i5284t[(to)2048cted from a moisture weight gain test using $_{sat}$ measurement data and extrapolated to the 100% RH. This is a low-bound e4n.8ction since the moisture will be usually in the mixture of water and vapor in free-volumes. The free volume fraction is usually between 1% and 5% for various packaging [28].

6. Hygroscopic swelling measurement

There are a number of experimental techniques for the charac508.421.42-1.316Td[(terization)-347(of)-352(hygroscopic)-346(swelling)-353(of though polymers exhibit viscoela4n.city under hygrothermal aging. In this study, silicon/underfill/FR-4 assemblies were prepared as shown in Fig. 11 [10]. The purpose of the study was to inve4n.gcte the hygroscopic swelling behavior of underfill in a flip-chip assembly were 8 mm ( ) × 5 mm ($_{41}$) × 1.8 mm ( ). The thickness of the underfill was 0.5 mm. A pre-crack was prepared at the sili508.4213.541-1.309Td[(con/underfi)11(ll)-366 other purpose of study [10]. In this paper, only defor8ctionfields at the leftward ported. An integrcted muln.5functional micro-moiré in system was developed [10], by combining moiré in
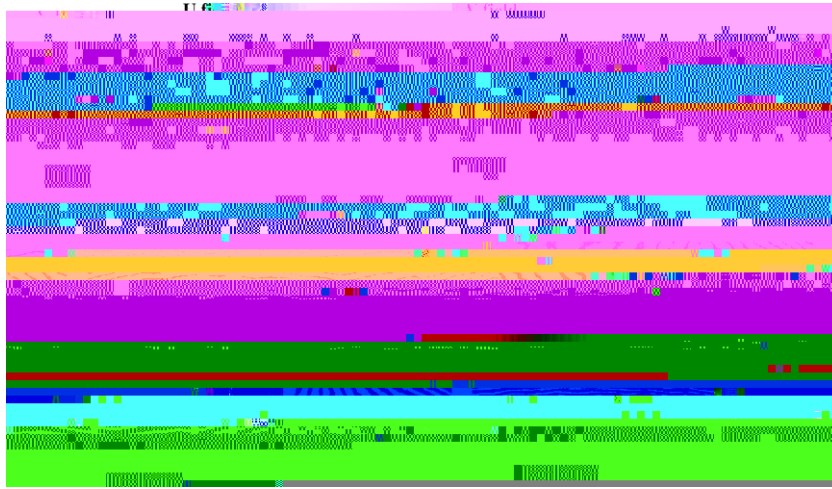
Fig. 12. Fringe patterns during hygrothermal aging under 85 °C/85% RH.
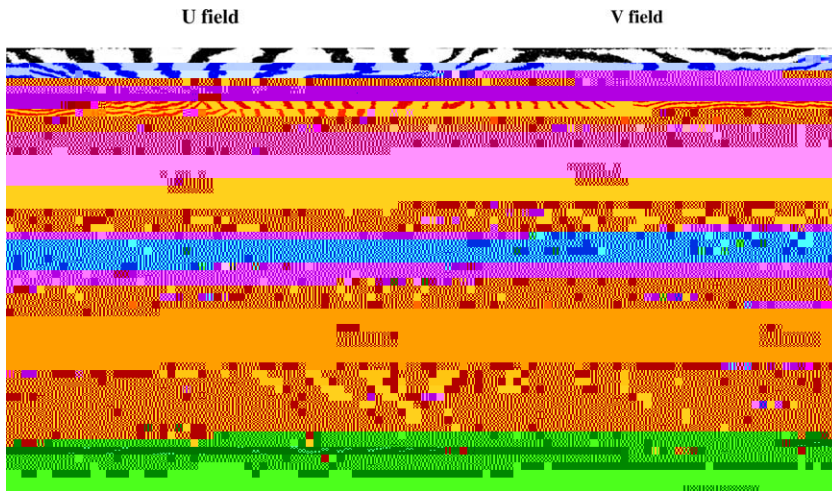
U field   V field

Fig. 13. Representative fringe patterns under the thermal aging test (85 °C).

energy is needed to break the hydrogen bond, and therefore, a higher temperature is needed. Zhou and Lucas [32] studied the mobility of water in different epoxy systems. The study shows that water molecules bind with epoxy resins through hydrogen bonding. Two types of bound water were found in epoxy resins. The binding types are classified as Type I or Type II bonding, depending on difference in the bond complex and activation energy. Type I bonding corresponds to a water molecule which forms a single hydrogen bond with the epoxy resin network. This water molecule possesses a lower activation energy and is easier to remove from the resin. Type II bonding is as a result of a water molecule forming multiple hydrogen bonds with the resin network. This water molecule, therefore, possesses a higher activation energy and is correspondingly harder to remove. Type I bound water is the dominant form of the total amount absorbed water. The amount of Type II bound water depends strongly on the exposure temperature and time. Higher temperature and longer exposure time result in a greater amount of Type II bound water.

7.2.

Consider the underfill tested for hygroscopic swelling, the volume change due to hygroscopic swelling based on the test data under 85 °C/85% was determined as [33]

$$\frac{\Delta}{} = 0.3\% \tag{22}$$

where is the total volume of the sample, and Δ is the volume change due to moisture absorption at a constant temperature.

On the other hand, if the material's free volume fraction is estimated as 3% as a representative value as follows

$$_0 = \frac{free\ volume}{} = 3\% \tag{23}$$

It reveals that the volume change by hygroscopic swelling is only a small fraction of the total free volume. In the previous section, the estimate of the free volume fraction does not consider the effect of hygroscopic swelling. This example inferred that the estimate of free volume fraction using weight gain data without considering the material swelling give a good approximation if the material does not swell excessively. Eqs. (22) and (23) indicate that the majority of moisture absorption does not contribute to the material's swelling.

It has been suggested that swelling is caused by water molecules bound to the polymer matrix and not by the free water molecules. Because the water molecule is polar, it is capable of forming hydrogen bonds with hydroxyl groups, thereby disrupting inter-chain hydrogen bonding with the net effect of increasing the inter-segmental hydrogen bond length. This concept has been

where $^{bound\ water}$ is the moisture mass for the bond formation per unit volume.

7.3.

Many polymer materials used in electronic packaging consist of fillers. While most fillers are not used with the intent of altering the sorption and transport of water within polymer, this concomitant effect is almost always unavoidable. Much of the effect of the fillers on the transport properties within the matrix is governed by the degree of interaction between the polymer matrix and the filler at the interphase. In most composites, it is desirable to have a strong adhesive bond between the two materials. The adhesive bonds can be of either a physical or physicochemical nature. Variations in the strength and nature of these bonds lead to three typical situations at the polymer/filler interface [36].

If the bonds are physical, water can be prevented from reaching the interfacial region and the amount of water absorbed depends only on the epoxy fraction of the composites. If physicochemical bonds, such as hydrogen bonds, are involved, the polymer may find its movement restricted in the vicinity of the filler. If this attraction is strong enough, a portion of the polymer matrix as well as the filler volume may be impermeable to the penetrating moisture.

If poor bonding exists at the interface, water transport may be enhanced by pathways open along the interface. In this case, the water is transported in the liquid state by capillary forces. Similar capillary transport may occur if microcracks and/or defects are present in the bulk of epoxy. Voids at the interface may increase the Langmuir sites of the composites, allowing higher equilibrium sorption. Water clustering in these voids can cause positive deviations from Henry's law [37].

The effect of interfacial bonding can be taken into account by comparing diffusion and sorption in neat polymer resins and composites. If, after correcting for the fiber content of the composite, there is no difference between the two, interphase effects may be negligible. This in general is found for glass/epoxy systems [38].

8. Governing equations for a deforming polymer with moisture considering phase transition

The phenomenological aspect of moisture-induced damage can be found in the works of Fan et al. [39], Hui et al. [40], Roy et al. [41,42], Rajagopal [43], and Sullivan and Stokes [44]. These authors have studied the coupled effect of polymer damage with moisture diffusion. However, a complete mathematical formulation on polymeric solids coupled with the thermodynamics of evaporation of moisture has not been developed. In this section the governing equations for a deforming polymer with moisture are developed. The general case of the moisture phase transition is considered. The governing equations are developed on the lines of soil or rock mechanics with multiphase flow. The solid phase is assumed to comprise a porous skeleton of polymers surrounded by moisture. The moisture flow is neglected here, while an all-round vapor pressure is exerted on the solid phase. The small strain theory is considered here for clarity, but the theory can be extended to large-deformation case. It is assumed that a vapor pressure by moisture, i.e., , causes only a uniform, volumetric strain by compressing the solids and that the major deformation of the porous skeleton is governed by the effective stress $\boldsymbol{\sigma}'$. This is defined as follows, with the sign convention that tension is positive,

$$\boldsymbol{\sigma} = \boldsymbol{\sigma}' - \mathbf{m} \tag{26}$$

where $\boldsymbol{\sigma}$ is the total stress and $\mathbf{m}$ is equal to unity for the normal stress components and zero for the shear stress components. At each point in the domain, the variables are in fact average values

observed through spectroscopic methods [34,35]. If such a postulation holds true, the hygroscopic swelling development would include two stages, which correspond to dual-stage moisture absorption theory. In the stage one, the absorption of water molecules take places in free-volumes or nano-voids, which is a reversible process. This stage would not contribute the hygroscopic swelling significantly. In the second stage, the hydrogen bonding is formed between the water molecules and polymer chains, which will cause the material's swelling.

In order to characterize the swelling behavior, the coefficients of hygroscopic swelling (CHS) is often introduced as follows

$$\varepsilon_{\text{swelling}} = \beta \tag{24}$$

where β is the coefficient of hygroscopic swelling and   is the moisture concentration. According to the above analysis, the formation of hydrogen bond with polymer materials causes the hygroscopic swelling of material, while the unbound water liquid/vapor fills in free-volumes, which does not cause swelling if the vapor pressure is low at lower temperatures. Therefore, the above equation might need to be modified if only a small fraction of moisture is responsible for the swelling of material. Instead of using the total moisture concentration in Eq. (24), the moisture concentration fraction which forms the hygro bonding (Type II) may be used.

$$\varepsilon_{\text{swelling}} = \beta\ ^{bound\ water} \tag{25}$$

over a representative elementary volume (REV) around any considered point in the porous medium domain. As long as the REV is independent of time and of location in the porous medium, the averaged equations obtained are independent of the geometry of the REV. The volume   of a REV is composed by the sum of the volume of solid phase and free volume

$$ = \ _{,} + \qquad\qquad\qquad (27)$$

where   is solid phase volume and   is the free volume. The (averaged) total stress vector at macroscopic level may be expressed in terms of intrinsic phase averages

$$\langle \boldsymbol{\sigma} \rangle = \frac{1}{ } \int \sigma \quad = \frac{1}{ } \left[\int \sigma \quad + \int \sigma \quad \right]$$
$$= \frac{\ }{ } \langle \sigma_{,} \rangle + \frac{\ }{ } \left[\frac{1}{ } \langle \sigma \rangle \right] \qquad\qquad (28)$$

where

$$\langle \sigma_\pi \rangle^\pi = \frac{1}{\pi} \int \sigma_\pi \qquad\qquad\qquad (29)$$

which, presents the average over one-phase. Then we have

$$\langle \boldsymbol{\sigma} \rangle = (1 - \ )\langle \boldsymbol{\sigma} \rangle \ - \ \mathbf{m}\langle \ \rangle = \boldsymbol{\sigma}' - \mathbf{m}\langle \ \rangle \qquad (30)$$

This is how we obtained Eq. (26). For clarity, we do not use the symbol <>, but one should always keep in mind that the quantities are in average at macroscopic level. In Eq. (30),

$$\boldsymbol{\sigma}' = (1 - \ )(\langle \boldsymbol{\sigma} \rangle \ + \mathbf{m}\langle \ \rangle) \qquad\qquad (31)$$

is the strain-producing stress in the solid skeleton, the effective stress. According to Terzaghi's definition it the sum of the pressure and average stress in the solid phase.

The constitutive equation relating this effective stress to the strains of the skeleton is now independent of the vapor pressure